ISSN 0869-5911, Petrology, 2020, Vol. 28, No. 3, pp. 287–300. © Pleiades Publishing, Ltd., 2020.
Russian Text © The Author(s), 2020, published in Petrologiya, 2020, Vol. 28, No. 5.

Oxygen Isotope Fractionation between Phenocrysts and Melt: Equilibrium Estimation for the Alkaline Lavas of Changbaishan Volcano (Northeast China)

E. O. Dubinina[a], *, O. A. Andreeva[a], A. S. Avdeenko[a], I. A. Andreeva[a], and Ji Jianqing[b]

[a] *Institute of Geology of Ore Deposits, Petrography, Mineralogy and Geochemistry (IGEM), Russian Academy of Sciences, Moscow 119017, Russia*

[b] *School of Earth and Space Sciences of Peking University, 100871, Beijing, China*

**e-mail: elenadelta@gmail.com*

Received August 2, 2019; revised September 8, 2019; accepted September 27, 2019

Abstract—The mechanisms of the occurrence of nonequilibrium oxygen isotope fractionation between olivine and plagioclase phenocrysts and the groundmass of rocks (from alkaline basalts to alkaline rhyolites) of Changbaishan volcano are considered. The basaltic trachyandesite–trachyte–comendite–pantellerite rock series shows a systematic increase of the $\delta^{18}O$ values of feldspar (from 5.4 to 7.8‰) and the rock groundmass (from 5.6 to 7.1‰). In contrast, the $\delta^{18}O$ values of olivine decrease from 5.35‰ typical of mantle peridotites to significantly lower values (3.88–4.14‰). This is accompanied by changes in olivine composition from the Mg-rich (*Fo* = 74–79) to almost pure fayalite (*Fo* = 1), thus indicating a positive correlation between the Mg-number and $\delta^{18}O$ of olivine. It is shown that feldspar and the rock groundmass are close to the oxygen isotopic equilibrium, whereas olivine–rock groundmass and olivine–feldspar pairs did not approach the oxygen isotopic equilibrium. The main mechanisms leading to the oxygen isotopic disequilibrium in the mineral–melt system are considered. An approach to the estimation of oxygen isotope equilibrium between the phenocrysts and melts is proposed. It takes into account the degree of melt polymerization (NBO/T ratio). This approach makes it possible to explain the positive correlation between $\delta^{18}O$ values and olivine Mg-numbers in the Changbaishan lavas, as well as the occurrence of low $\delta^{18}O$ values (down to +3‰) in ferrous olivine from alkaline–salic rocks. The $\delta^{18}O$ values observed in the olivine and the rock groundmass reflect changes in the degree of melt polymerization during crystal fractionation. The proposed model does not require an additional geological process, in particular, the contribution of a low–$\delta^{18}O$ material in the formation of the Changbaishan differentiated rock series.

Keywords: oxygen isotope fractionation, phenocryst, melt, olivine, plagioclase, NBO/T, differentiation, Changbaishan volcano

DOI: 10.1134/S0869591120030030

INTRODUCTION

Estimation of oxygen isotope equilibrium between phenocrysts and groundmass is a topical problem in the oxygen isotope geochemistry of porphyritic rocks. The phenocryst–melt system is thought to be close to equilibrium due to the high diffusion rates (Farver, 2010; Lesher, 2010, and others) and low oxygen isotope fractionation coefficients, which are typical of most silicate melts and minerals at high temperatures (Bigeleisen and Mayer, 1947; Chacko et al., 2001; Clayton and Kieffer, 1991). Mantle melts usually reach isotopic equilibrium, whereas melts that experienced further evolution frequntly record a complete oxygen isotopic disequilibrium between phenocrysts and groundmass (Bindeman et al., 2008; Genske et al., 2013). For instance, disequilibrium is frequently observed between olivine phenocrysts and host matrix in mafic and ultramafic rocks, which is interpreted as reflecting the isotope equilibrium between olivine and mantle melts of earlier stages (Day et al., 2014; Genske et al., 2013; Günther et al., 2018). It should be noted that the estimates of the degree of isotopic equilibrium in the phenocryst–melt system are based on a few experimental data (Muehlenbachs and Kushiro, 1974; Appora et al., 2003), empirical considerations (Eiler, 2001; Kalamarides, 1986), and semiempirical calculation (Zhao and Zheng, 2003). The absence of systematic data on the phenocryst–melt equilibrium oxygen isotope fractionation coefficients makes it impossible to establish unambiguously whether equilibrium between phenocrysts and groundmass has been attained.

The oxygen isotopic nonequilibrium between phenocrysts and melt can be explained by the local equilibrium crystallization of mineral from a melt, which, regardless of crystallization, shows a change in $\delta^{18}O$ owing to the contamination, advanced crystallization differentiation, or other processes (DePaolo, 1981; Taylor, 1980). To make this mechanism work, it is necessary to prevent the attainment of complete (throughout the entire crystal) isotopic equilibrium throughout the entire crystal with a change of isotopic composition of crystallization environment. This could be provided either by isolation of crystalline phase from isotope exchange owing to its removal or by low oxygen diffusion rate in mineral (Dubinina and Lakshtanov, 1997). Thus, such thermally stable minerals as olivine or zircon (Valley, 2003; Cherniak and Watson, 2003; Gérard and Jaoul, 1989; Chakraborty, 2010) frequently demonstrate a complete isotopic nonequilibrium with surrounding minerals or melt during rapid cooling (Dodson, 1973; Giletti, 1986; Valley, 2001).

The oxygen isotopic nonequilibrium between phenocrysts and groundmass at rapid cooling could be observed even for minerals with high diffusion rates. For instance, felsic volcanic rocks of the Caucasian Mineral Water (CMW) region show a characteristic correlation of $\delta^{18}O$ values of feldspar and phlogopite phenocrysts with those of the groundmass, which is caused by the contamination of the melt by carbonate material (Dubinina et al., 2010). It was shown that the absence of internal isotopic equilibrium in the porphyritic rocks of the CMW laccoliths was caused by the rapid cooling rate and the high water activity in the melt.

The absence of complete isotope equilibrium between a melt and a mineral could be caused by the rapid change of the crystal–melt fractionation coefficient at rapid temperature decrease or a change of the melt composition during differentiation. In the latter case, the nature of isotope shift is difficult to determine, because the chemical composition of melt significantly changes and its structure becomes more polymerized at high degree of differentiation. A change in the degree of polymerization could cause isotope effects, as observed in experiments (Borisov and Dubinina, 2014; Dubinina and Borisov, 2018).

This paper is dedicated to the detailed consideration of oxygen isotopic relations between phenocrysts and groundmass in the differentiated rock series. The aim of the work is to estimate the degree of complete oxygen isotope equilibrium and to determine mechanisms determining the $\delta^{18}O$ relations in the phenocryst–melt system. To this end, we need rock association that is characterized by (1) the extremely wide compositional range from basic to felsic varieties, without significant traces of contamination; (2) the high cooling rates of melts to exclude the retrograde isotope exchange; (3) the presence of common phenocryst minerals containing in all rocks, preferably, with the low oxygen diffusion rate.

These requirements are met by the alkaline lavas of Changbaishan volcano located at the China–North Korea boundary. The volcano lavas vary from trachybasalts to alkaline rhyolites and show no traces of significant crustal contamination (Hsu et al., 2000; Fan et al., 2007; Sakhno, 2007, 2008; Andreeva et al., 2018). Specifics of the mineral composition of Changbaishan volcanic rocks caused by their high alkalinity and Fe mole fraction consists in the ubiquitous presence of phenocrysts of olivine of different Mg–number (*Fo* (mol % of forsterite) varies from 78–79 to 1) and feldspar (from plagioclase (An_{74}) to anorthoclase ($An_{0.3}$)) (Andreeva et al., 2018) in all rocks of the volcano. Thus, all types of derivatives of the Changbaishan magmatic system contain phenocrysts of two minerals with contrasting diffusion characteristics: olivine and plagioclase. For instance, the rate of oxygen diffusion in plagioclase at 1000°C could be approximately five orders of magnitude higher than that in olivine (Giletti et al., 1978; Farver and Yund, 1990; Jaoul et al., 1980; Chakraborty, 2010).

The geochemical studies of the rocks of Changbaishan volcano showed that the primary melts of the magmatic series were high–Ti basaltic magmas of elevated alkalinity. Their source was close to the ocean island mantle (OIB) with high Ba and P_2O_5 concentrations, which are caused by the interaction between mantle plume and subducted slab (Kuritani et al., 2011; Andreeva et al., 2018). The study of melt inclusions in minerals of the entire rock series allowed us to trace the evolution of magmatic melt from basic rocks to comendites and pantellerites, which are sharply enriched in trace elements (Th, Nb, Ta, Zr, REE) (Andreeva et al., 2018). These studies showed that the formation of this volcanic series was controlled by the crystallization differentiation of parental basaltic magmas in shallow (13–3.5 km) magma chambers within a wide range of temperature (from 1220 to 700°C) and pressure (from 3100 to 1000 bar). The Sr and Nd isotopic study of the trachybasatic andesites, trachytes, comendites, and pantellerites of Changbaishan volcano (Liu et al., 1998, 2015; Andreeva et al., 2018) indicates that felsic rocks and basalts are similar in Nd isotopic composition, but differ in Sr isotopic composition. The correlation of $^{87}Sr/^{86}Sr$ ratio with $^{87}Rb/^{86}Sr$ suggests the accumulation of radiogenic Sr in a melt with a high Rb/Sr ratio over a short geological time (Andreeva et al., 2018).

Presented data suggest that the unique characteristics of the alkaline volcanic rocks of Changbaishan volcano can be used to trace the evolution of oxygen isotope compositions of phenocrysts and groundmass within a single highly differentiated series and to decipher mechanisms responsible for the observed oxygen isotope relations in the phenocryst–melt system.

SAMPLES AND METHODS

The studied samples represent the end members of the differentiated series of Changbaishan volcano. Changbaishan volcano is the largest volcano within the eponymous volcanic area (>15000 km^2). It is located at the northern margin of the Archean–Proterozoic Sino–Korean craton, being constrained to the intersection of the NE–trending Tan–Lu rift system and NW–trending Paektusan fault system (Liu et al., 2015; Sakhno, 2008; Andreeva et al., 2014, 2018). In addition to basaltic lavas, the volcano produced large–scale felsic eruptions (Yarmolyuk et al., 2011): its 2700-m high cone consists mainly of alkaline–salic rocks enriched in trace elements (Th, Nb, Ta, Zr, REE). The volcano was formed in several stages, including fissure eruptions of shield volcano at the base of buildup and the growth of cone (2.77–0.31 and 0.52–0.02 Ma, respectively; Wei et al., 2007a, 2007b), as well as the caldera stage related to the great explosion at 946 A.D. (Oppenheimer et al., 2017), and modern post-caldera stage (Wei et al., 2007). The basalt–trachybasalt–trachybasaltic andesite lavas were formed at the shield stage, while the cone and caldera are made up mainly of alkaline salic rocks: trachytes, comendites, and pantellerites.

Alkali basalts that compose the shield volcano and caldera (samples B–10 and BT–2) are also geochemically similar (Andereeva et al., 2018). They have high-Ti (TiO_2 up to 2.9 wt %), Fe-rich (Fe_2O_{3tot} up to 9.8 wt %), high–alumina (Al_2O_3 up to 17.8 wt %) composition with the high contents of alkalis (up to 6.9 wt %) and P_2O_5 (up to 0.7 wt %) Table 1). The rocks are characterized by the low REE contents and significant LREE enrichment relative to HREE ($(La/Yb)_N$ = 12–14), enrichment in Ba (up to 1020 ppm in trachybasaltic andesite B–10) and depletion in Th and U (< 10 ppm each). The alkali contents increase from basalts to trachytes. A further increase of SiO_2 content from trachytes to pantellerites and comendites is accompanied by an insignificant decrease of total alkalis (Na_2O + K_2O) and contents of some major oxides: Al_2O_3, FeO_{tot}, MgO, TiO_2, CaO, P_2O_5 (Table 1).

The alkaline–salic rocks (samples BT-26, BT-2b, and BT-3) have similar geochemical characteristics. The $(La/Yb)_N$ ratio is 8–13, Eu/Eu* < 0.06. These rocks have high REE contents reaching 1000 ppm (Andreeva et al., 2014, 2018), extremely high Zr content (up to 2340 ppm), and the low contents of Ba (up to 12 ppm) and Sr (< 5 ppm). Trachytes show SiO_2 variations from 62 to 69 wt % at insignificant variations of Na/K ratio and total alkalis 10–11.3 wt % (Table 1).

The oxygen isotopic studies were carried out in the end member varieties of the differentiated series—alkaline basaltic and alkaline–salic rocks, which are represented by coarsely porphyritic varieties of trachybasaltic andesites, trachytes, comendites, and pantellerites taken from the southern slope and within the shield buildup of Changbaishan volcano (Fig. 1).

Table 1. Composition of alkaline lavas of Changbaishan volcano

Component	B-10	BT-2	BT-26	BT-2b	BT-3
SiO_2	52.18	52.37	67.48	71.88	70.18
TiO_2	2.87	2.25	0.42	0.24	0.33
Al_2O_3	16.33	17.82	14.19	10.79	11.27
FeO	9.77	8.64	5.69	4.44	5.88
MnO	0.14	0.11	0.13	0.08	0.12
MgO	3.89	4.17	0.2	0.19	0.17
CaO	6.63	7.24	0.91	0.37	0.46
Na_2O	4.13	4.23	6.07	5.19	6.14
K_2O	2.8	2.35	4.9	4.28	4.58
P_2O_5	0.66	0.41	0.03	0.02	0.03
L.O.I.	0	0.37	0.03	2.15	0.71
Total	99.4	99.95	100.06	99.63	99.87
NBO/T*	1.009	1.118	0.127	0.112	0.135

* The NBO/T ratios were calculated using the equations from (Mysen, 1990).

Sample Description

Trachybasaltic andesite sample (sample B-10) taken within the shield base of the volcano is a coarsely porphyritic rock (Fig. 2a) with olivine, plagioclase, and less common clinopyroxene (augite) phenocrysts. Subeuhedral olivine is ca. 0.5–1 mm in size, shows no zoning, and has a relatively high-Fe composition (*Fo* = 72–76.5, Table 2). Plagioclase phenocrysts are represented by prismatic, more rarely, tabular crystals 0.5–7 mm in size, of labradoritic composition ($An_{61–69}$, Table 2). The groundmass consists of high-Ti augite (TiO_2 = 1.5–3.2 wt %), low-Mg olivine (*Fo* = 50–62), moderate- and high-Ca plagioclase ($An_{68–73}$), titanomagnetite, ilmenite, and residual glass of trachytic composition.

The trachybasaltic andesite from the southern surrounding of the caldera (sample **BT–2**) is represented by scoria. The rock has a porphyritic texture (Fig. 2b) and contains olivine, plagioclase, and extremely rare clinopyroxene phenocrysts. The olivine phenocrysts form 0.1–0.3 mm subeuhedral crystals of high-Mg composition (*Fo* = 78.1–79.1) (Table 2). The plagioclase occurs as prismatic crystals complicated by polysynthetic twins from 0.5 to 1 mm long. In composition, it corresponds to bytownite (An_{74}, Table 2). The groundmass is partially devitrified and consists of parallel oriented plagioclase lamellae ($An_{61–74}$), interstices between which are filled with clinopyroxene (Ti-augite), olivine (*Fo* = 44.6–45.5), titanomagnetite, ilmenite, apatite, and trachyandesite–trachyte glass.

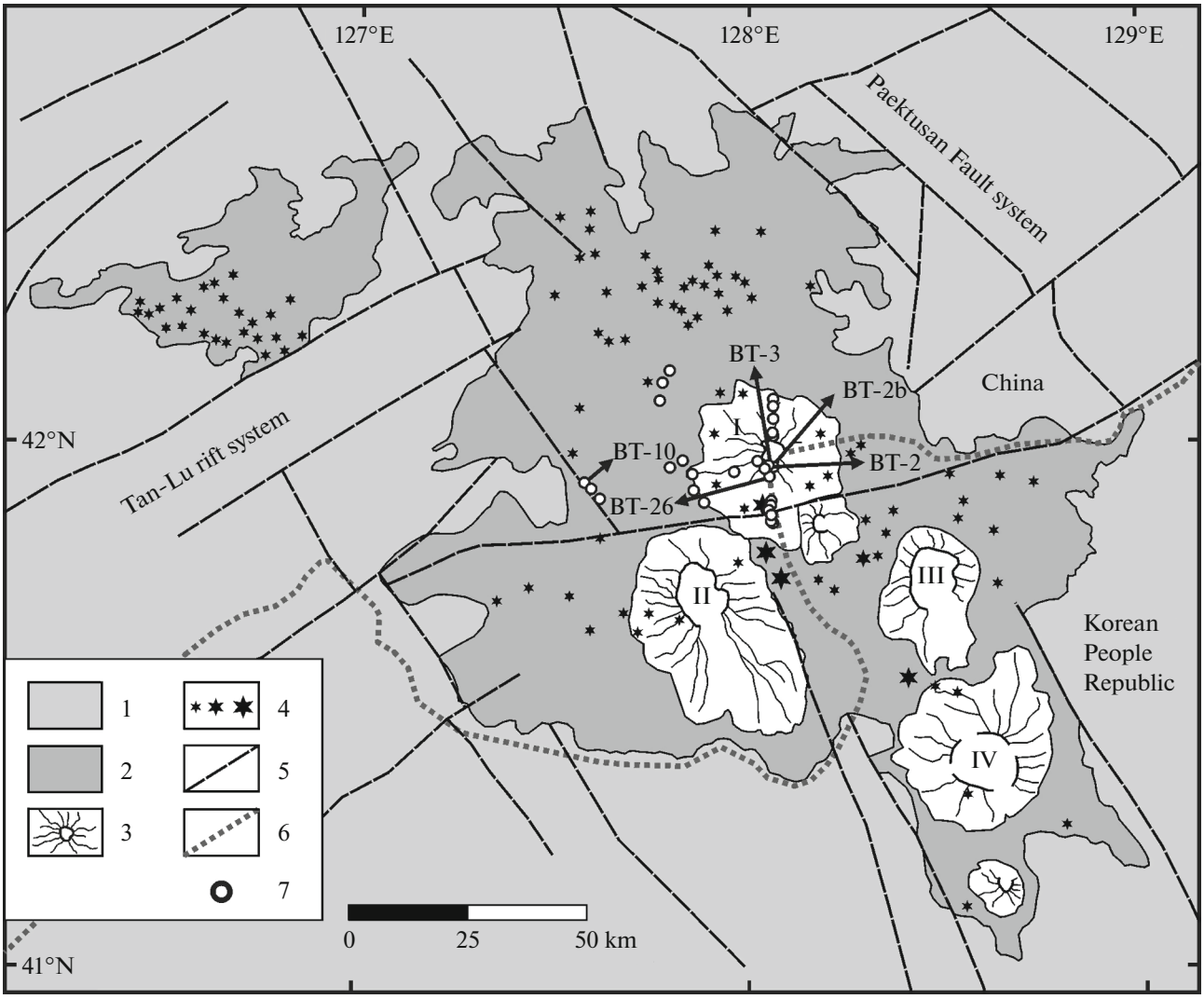

Fig. 1. Map of the Changbaishan volcanic area. (1) Host rocks; (2) volcanic complex of the shield stage (Miocene–Early Pleistocene), (3) stratovolcanoes of the caldera stage, Pliocene–Holocene ((I) Changbaishan, (II) Wangtian'e, (III) Northern Baotaishan, (IV) Southern Baotaishan); (4) small volcanic cones, diatremes, and volcanic domes, (5) faults, (6) state boundary, (7) sampling localities.

Trachytes collected on the southern slope of the volcano (sample BT-26) are porphyritic rocks (Fig. 2c) containing up to 20% anorthoclase phenocrysts and subphenocrysts of fayalite and clinopyroxene (hedenbergite). These rocks are dominated by anorthoclase ($An_{1.5–2.3}$) (Table 2), which forms transparent prismatic crystals ca. 4–5 mm, sometimes reaching 1 cm in length. Olivine in these rocks is represented by practically pure fayalite (Fo = 2.1–3.7) (Table 2), which occurs as subeuhedral tabular yellowish–brown crystals up to 0.1 mm in size. The MgO content is less than 1.4 wt %. Hedenberite phenocrysts are small (0.2–0.4 mm), tabular, sometimes, xenomorphic green crystals. The groundmass is made up of aggregate of anorthoclase, hedenbergite, quartz, sometimes, arfvedsonite. Accessory minerals are ilmenite and titanomagnetite.

Comendite sample is represented by pumice collected in the surrounding of the southern part of the caldera (sample BT–2b) and also has a porphyritic texture. Phenocrysts comprise mainly anorthoclase and scarce sanidine. Subphenocrysts of fayalite and clinopyroxene (ferrohedenbergite) are less common. The anorthoclase ($An_{0.1–0.6}$) (Table 2) is observed as short–prismatic and tabular crystals 1–4 mm in size. It has the high FeO content up to 0.3–0.6 wt %. The sanidine occurs as colorless tabular crystals 0.2–0.4 mm in size. The fayalite subphenocrysts 0.1–0.2 mm in size form subeuhedral tabular crystals with smoothed edges. The MgO content in the fayalite (Fo = 12.7) is no more than 8 wt % (Table 2). The groundmass is loose and consists of a glass and microlites of clinopyroxene (ferrosalite), alkali amphibole (edenite), titanomagnetite, and fluorapatite contain-

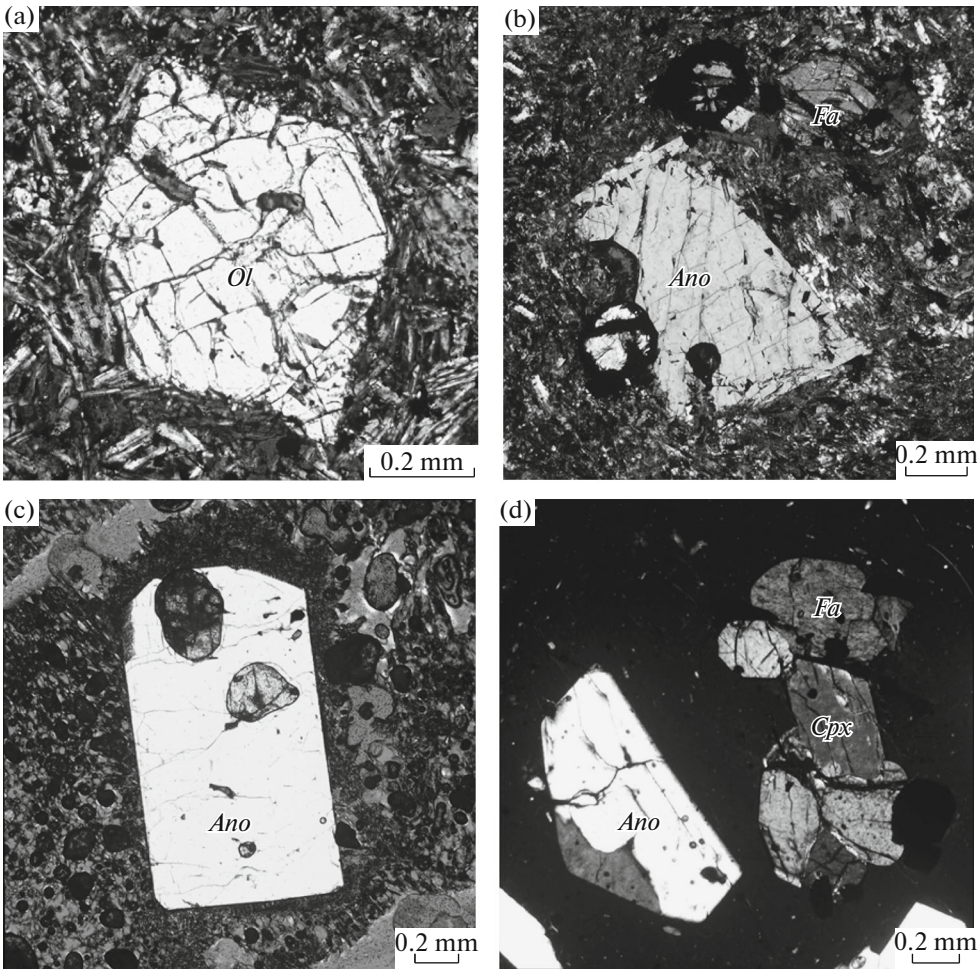

Fig. 2. Photo of polished thin sections: (a) trachybasaltic andesite, sample B-10, (b) trachyte, sample BT-26, (c) comendite, sample BT-2b, (d) pantellerite, sample BT-3. (*Ol*) olivine, (*Fa*) fayalite, (*Ano*) anorthoclase, (*Cpx*) clinopyroxene.

ing up to 15–20% britholite (Fig. 2d). The groundmass has an agpaitic (agpaitic coefficient, *K*a = 1–1.1) trachyte–rhyolite composition.

Pantelleritic ignimbrite (sample BT-3) was also collected in the southern surrounding of the caldera. Phenocrysts include anorthoclase, fayalite, less common ferrohedenbergite and quartz. The anorthoclase ($An_{0.3}$) (Table 2) forms 3–4 mm columnar crystals. The fayalite (*Fo* = 0.8–1) is practically devoid of MgO (< 0.4 wt %, Table 2), while the FeO content reaches 66 wt %. It is represented by 0.2–0.4 mm bright yellow crystals. The rock has an eutaxitic structure, with glass consisting of pantellerite groundmass. Accessory minerals are REE fluorapatite, titanomagnetite, ilmenite, pyrite, and cupriferous pyrite (Fig. 2d).

Oxygen Isotope Analysis

The chemical composition of rocks and minerals was studied previously at the IGEM RAS (Moscow) using X-ray fluorescence, ICP-MS, and microprobe analysis. These results together with detailed description of analytical techniques are given in (Andreeva et al., 2014, 2018).

In samples analyzed for oxygen isotope composition, we previously studied major-, trace-, Sr–Nd composition and melt inclusions. The oxygen isotope composition was studied in thoroughly picked olivine and plagioclase phenocrysts and groundmass represented by either glass or finely crystalline aggregate. The analysis was carried out by laser fluorination (Sharp, 1990) at the Laboratory of Isotope Geochemistry and Geochronology of IGEM RAS. The error in $\delta^{18}O$ determination was ±0.1‰. The results given in per mil relative to V-SMOW standard were controlled by measurements of NBS 28 (quartz) and UWG 2 (garnet) standards (Valley et al., 1995). The technique is described in detail in (Dubinina et al., 2015).

Table 2. Oxygen and modal composition of phenocrysts (*Ol*, *Pl*) and groundmass of alkaline lavas of Changbaishan volcano

Sample number	*T*, °C*	*T*(*Pl*–*Ol*)**	*Fo*(*Ol*)	*An*(*Pl*)	$\delta^{18}O$(*Pl*), ‰	$\delta^{18}O$(*Ol*), ‰	$\delta^{18}O$(*m*), ‰
B-10	1180	1600	74.5 (72–77)	65 (61–69)	5.92	5.34	5.64
BT-2	1200	1670	78.5 (78–79)	74	5.87	5.35	5.81
BT-26	1050	800	3 (2–4)	1.9 (1.5–2.3)	6.24	3.88	6.44
BT-2b	700	670	12.7	0.4 (0.1–0.6)	7.22	4.14	6.90
BT-3	1020	560	0.9 (0.8–1)	0.3	7.84	3.88	7.09

* Determined by MI study, accuracy of ±10°C. ** Calculated using the isotope geothermometers (Chacko et al., 2001).

RESULTS

The $\delta^{18}O$ values in the olivine ($\delta^{18}O$(*Ol*)) and plagioclase ($\delta^{18}O$(*Pl*)) phenocrysts, as well as in the groundmass of trachybasaltic andesite, trachyte, comendite, and pantellerite ($\delta^{18}O$(*m*)) from Changbaishan volcano are listed in Table 2. The lavas show a systematic increase of $\delta^{18}O$(*m*) (from 5.6–5.8 to 6.4–7.1‰) from alkali basalts to alkali rhyolites (Table 1). The $\delta^{18}O$ value of plagioclase increases in the same direction (from 5.4 to 6.2–7.8‰), being close to that of the groundmass. The $\delta^{18}O$ value of high-Mg olivine (*Fo* = 74–79) from alkali basalts (5.34–5.35‰) corresponds to the upper limit of values established for olivines from mantle peridotites (5.14 ± 0.24‰; Mattey et al., 1994). The $\delta^{18}O$ value of fayalite (*Fo* = 15–1) from alkali rhyolites is much lower than mantle values (3.88–4.14‰). Thus, the values of $\delta^{18}O$(*m*) increase from alkali basalts to alkali rhyolites, while $\delta^{18}O$(*Ol*) decrease (Fig. 3). The Fe mole fraction increases in the same direction, thus showing a negative correlation between $\delta^{18}O$(*Ol*) and Fe mole fraction or a positive correlation between $\delta^{18}O$(*Ol*) and Mg-number of olivine.

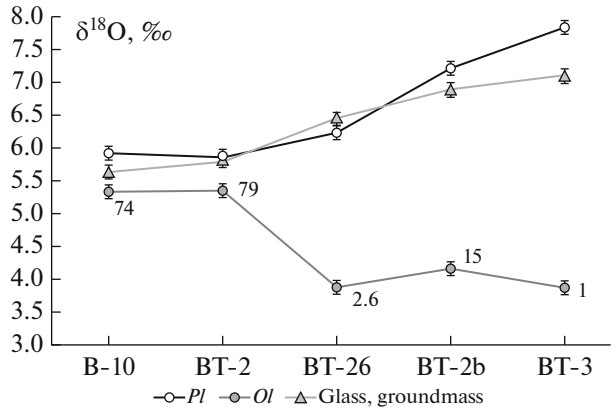

Fig. 3. Oxygen isotope composition of plagioclase, olivine, and matrix (glass, groundmass). Numbers show the content of forsterite end member in olivine (*Fo*).

All studied samples demonstrate an expressed oxygen isotopic nonequilibrium between olivine phenocrysts and groundmass and between phenocrysts of olivine and plagioclase. Unrealistic temperature (Table 2) estimates were obtained from plagioclase–olivine pair (Chacko et al., 2001): extremely high for alkali basalts and extremely low for alkali rhyolites (Table 2). A good agreement between calculated temperatures and those obtained from melt inclusions (Andreeva et al., 2018) for comendite BT-2b was likely occasional.

DISCUSSION

Estimation of Complete Oxygen Isotope Equilibrium between Phenocrysts and Groundmass

The study revealed a complete oxygen isotope disequilibrium between groundmass and olivine phenocrysts. It is possible that plagioclase phenocrysts are also in disequilibrium with groundmass, which can be roughly estimated by calculation. The $\delta^{18}O$ values of plagioclase and olivine phenocrysts corresponding to the isotopic equilibrium with groundmass were calculated with allowance for a change of major element composition from trachybasaltic andesite to comendite and pantellerite during differentiation.

The oxygen isotopic fractionation in rock-forming minerals was well studied, but there are insufficient data on the oxygen isotopic fractionation in silicate melts of different composition. The experimental estimates of equilibrium fractionation coefficients for melts are fragmentary (Kyser et al., 1998; Lester et al., 2013; Stolper and Epstein, 1991; Palin et al., 1996; Matthews et al., 1994; Appora et al., 2003), while theoretical calculations are absent due to the poor study

Table 3. Oxygen isotope equilibrium fractionation between the phenocryst and melts calculated using the $I^{18}O$ index (Zhao and Zheng, 2003)

$10^3 Ln\ \alpha$ (*Pl*–L)*	B-10	BT-2	BT-26	BT-2b	BT-3
$10^3 Ln\ \alpha$ (*Pl*–L) measured data	0.28	0.06	–0.21	0.32	0.75
$10^3 Ln\ \alpha$ (*Ol*–L) measured data	–0.30	–0.46	–2.56	–2.76	–3.21
$I^{18}O$ index of rock (melt)	0.8465	0.8486	0.9085	0.9265	0.9148
$10^3\ Ln\alpha$ (*Pl*–L)*	0.04	–0.04	0.17	0.36	0.19
$10^3\ Ln\alpha$ (*Ol*–L)*	–0.94	–0.95	–1.31	–2.40	–1.38

* Calculated value.

of structure of silicate melts (Ariskin and Polyakov, 2008). Uncertainties in estimating the oxygen fractionation factors in melts are usually solved by approximation using either melt calculation for the normative mineral composition (Eiler, 2001; Bucholz et al., 2017) or geochemical indices, for instance, Garlick's index (Garlick, 1966) or semiempirical isotope index $I^{18}O$ (Zhao and Zheng, 2003). Approximation of melt by normative mineral composition with the calculation of weighted average fractionation coefficient for individual minerals is usually applied for basic melts (Eiler, 2001; Bindeman et al., 2008; Bucholz et al., 2017). As was shown in experiment, this approximation for basaltic glass is appropriate to predict oxygen isotope fractionation factors (Appora et al., 2003; Dubinina and Borisov, 2018). However, the recalculation of alkaline rocks for normative composition is an intricate problem and frequently gives exotic mineral assemblages, for which reliable isotope geothermometers are absent. For instance, the normative recalculation of pantellerite (sample BT-3) yields quartz–orthoclase–albite–acmite mineral assemblage, whereas the modal mineral composition of this sample comprises anorthoclase, fayalite, ferrohedenbergite, ilmenite, titanomagnetite, and REE apatite. Hence, this approach is not suitable for alkaline rocks. Instead, it is more appropriate to use geochemical indices, for instance, isotopic index $I^{18}O$ (Zheng, 1993), which can be used to calculate the oxygen isotope fractionation factors based on the major–component chemical composition of rocks (Zhao and Zheng, 2003). The value of the oxygen isotope index $I^{18}O$ was calculated from the major element rock composition presented in Table 1 for each sample. Isotope indices $I^{18}O$ for olivine phenocrysts were calculated as the weighted average from forsterite–fayalite end member proportions, while those for plagioclase phenocrysts, from albite–anorthite proportions of (Table 2). Temperature dependences of fractionation factors for pure end members of olivine (fayalite and forsterite) and plagioclase (albite and anorthite) were taken according to equations (Zheng, 1993). The calculation was made for temperatures determined from melt inclusion study in each sample (Table 2).

The calculation shows that the complete oxygen isotope equilibrium is clearly disturbed between olivine phenocrysts and the groundmass, and only minimally disturbed between plagioclase phenocryst and the groundmass, showing some deviations from calculated equilibrium values only for alkali rhyolites (Table 3, Fig. 4). The oxygen diffusion rate in plagioclase likely was sufficiently high to provide the equilibrium between this mineral and matrix of high–temperature (1180–1200°C, Table 2) alkali basalts. A decrease of crystallization temperature of alkali rhyolites (on average, by 150°C) could affect the oxygen diffusion rate in plagioclase and lead to a slight deviation of this mineral from equilibrium with the groundmass. Unlike plagioclase, the measured $\delta^{18}O$ values of olivine deviate to the opposite sides from the inferred equilibrium values. It is seen in Fig. 4 that olivine phenocrysts are beyond the complete equilibrium with groundmass both in alkali basalts and in alkali rhyolites.

The Disturbance of Complete Oxygen Isotope Equilibrium by the Local–Equilibrium Mechanism

The complete oxygen isotope equilibrium between olivine phenocrysts and melt could be disturbed by local isotope equilibrium between the surface of growing crystal and a melt and by the low oxygen diffusion rate in crystal during growth. If $\delta^{18}O$ values of melt and (or) mineral–melt fractionation coefficient change during crystal growth, the cores of mineral phenocryst with low diffusion rates could be in disequilibrium with the melt. This will result in a systematic correlation of oxygen isotope compositions between disequilibrium mineral and crystallization medium (Dubinina and Lakshtanov, 1997). According to the mass–balance equation, the oxygen isotope composition of initial melt prior to the onset of crystallization (δ_0) could be written as a sum:

$$\delta_0 = \delta_m (1 - m) + \overline{\delta_f} m, \quad (1)$$

where δ_m and δ_f are the oxygen isotopic compositions of the groundmass and phenocrysts, respectively, while m is the weight fraction of oxygen in phenocrys-

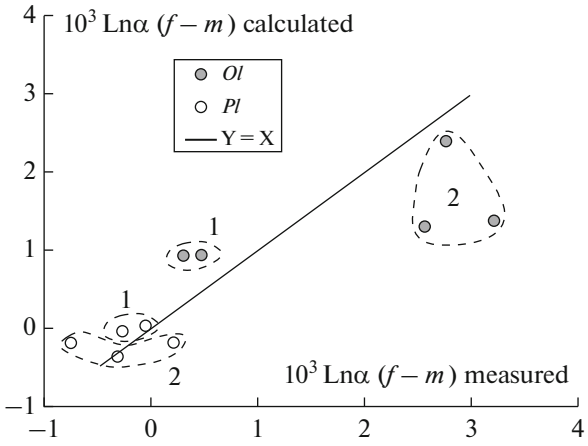

Fig. 4. Comparison of measured fractionation in the phenocryst–melt system in lavas of Changbaishan volcano with the equilibrium fractionation coefficients calculated through isotope index $I^{18}O$ (Zheng, 1993, Zhao and Zheng, 2003). Dashed outlines correspond to fields of alkali basalts (1) and alkali rhyolites (2).

tic mineral, and the overbar means the oxygen isotope composition averaged over the oxygen mass:

$$\overline{\delta_f} = \frac{1}{m}\int_0^m (\delta_m + \Delta_{f-m})dm. \quad (2)$$

In Eq. (2), the oxygen isotopic composition of crystallizing mineral at any moment of crystallization is given by the local equilibrium with a melt through an equilibrium oxygen isotope shift Δ_{f-m}. Combining Eqs. (1) and (2) differentiating with respect to m give equation describing a change of oxygen isotope composition of a melt:

$$\frac{d\delta_m}{dm} = -\frac{\Delta_{f-m}}{(1-m)}. \quad (3)$$

Assuming that the oxygen isotope composition of a melt (δ_m) at the beginning of crystallization ($m = 0$) equals the initial composition (δ_0), the Eq. 3 can be solved as:

$$\delta_m = \delta_0 + \mathrm{Ln}(1-m). \quad (4)$$

Combining this equation with mass balance equation (1) gives an integral (or averaged) oxygen isotope composition of mineral phenocrysts, which corresponds to $\delta^{18}O$ measured in sample by conventional oxygen isotopic analysis:

$$\overline{\delta_f} = \delta_0 + \left(1 - \frac{1}{m}\right)\Delta_{f-m}\mathrm{Ln}(1-m). \quad (5)$$

Eqs. (1)–(5) describes a system, ignoring a change in temperature (i.e., Δ_{f-m} value is constant) and simultaneous crystallization of two and more minerals. However, this calculation can be used to illustrate the direction and scale of inferred isotope shift in phenocrysts. A linear change of $\delta^{18}O(m)$ from 5.6 to 7.1‰ (i.e., within measured $\delta^{18}O(m)$) and a linear change of olivine and plagioclase proportions from $\{X_{Ol} = 0.6, X_{Pl} = 0.4\}$ in alkali basalts to $\{X_{Ol} = 0.1, X_{Pl} = 0.9\}$ in alkali rhyolites are given for calculation. The values of oxygen isotope fractionation for the olivine–melt and plagioclase–melt systems were taken to be constant and equal −1.1‰ and −0.1‰, respectively. Figure 5 demonstrates the observed variations of $\delta^{18}O$ values in olivine and plagioclase phenocrysts ($\delta^{18}O(f)$) in lavas of Changbaishan volcano relative to the oxygen isotope composition of groundmass, $\delta^{18}O(m)$. For comparison, this plot also shows the calculated variation curves of $\delta^{18}O(Ol)$ and $\delta^{18}O(Pl)$ corresponding to the complete equilibrium with melt (solid lines 1 and 3) and variation curves of these values when the local isotope equilibrium is fulfilled but complete diffusion equilibration between phenocryst and melt was not attained (dashed curves 2 and 4). A constant value was assumed for phenocryst–melt isotope fractionation, but variations of this value, as follows from Table 3, are insignificant, while calculated curves in Fig. 5 provide insight into direction and approximate value of expected isotope shifts in phenocrysts at local equilibrium disturbance of the complete oxygen isotope equilibrium. The measured $\delta^{18}O(Pl)$ values in Fig. 5 are grouped along the calculated curve of complete equilibrium with melt, although the plagioclase compositions tend to be shifted away from the equilibrium curve in the region of most evolved rocks. Nonetheless, the behavior of $\delta^{18}O(Pl)$ is well consistent with a scheme of diffusion-controlled oxygen equilibrium between growing plagioclase phenocryst and surrounding melt, which can be provided by the high oxygen diffusion rate in plagioclase and the low oxygen fractionation coefficient in the plagioclase–melt system (Table 3).

We would expect that the $\delta^{18}O(Ol)$ values would be grouped along curve describing the local equilibrium disturbance of the complete isotope equilibrium with melt (dashed line 4 in Fig. 5), because olivine has the low oxygen diffusion rates. However, the measured $\delta^{18}O(Ol)$ of alkali basalts deviate to the greater values, while $\delta^{18}O(Ol)$ of alkali rhyolites, to the lower values relative to theoretical curves (curves 3 and 4 in Fig. 5). The fact that the $\delta^{18}O(Ol)$ values are not described by the local–equilibrium model indicates the absence of not only complete, but also local equilibrium in the olivine–melt system, at least from the view point of available approaches to estimating the values of equilibrium oxygen isotope partitioning in the mineral–melt system.

Change of Olivine Mg–Number and Contamination by Low– $\delta^{18}O$ Material

The $\delta^{18}O(Ol)$ value decreases from basic to felsic varieties, whereas $\delta^{18}O$ in the groundmass increases. The olivine Mg-number decreases in the same direction and, hence shows a positive correlation with $\delta^{18}O$ value. Similar correlation was also observed in the differentiated basaltic series (Genske et al., 2013; Day et al., 2014; Wang et al., 2015; Nardini et al., 2009). The lavas of Changbaishan volcano show extremely wide variations of olivine Mg-number from 1 to ≈80 mol % forsterite (Table 2). It would be reasonable to explain this correlation by the influence of olivine composition on the olivine–melt oxygen isotope fractionation. However, the oxygen isotope shift related to the Mg–Fe substitution in olivine is insignificant. As follows from the temperature dependences of oxygen isotope fractionation for pure fayalite and pure forsterite (Zheng, 1993), the equilibrium fractionation between fayalite and forsterite in the high-temperature region is 0.19‰ at 800°C and 0.17‰ at 1200°C. Hence, significant shifts of $\delta^{18}O$ in olivine (by more than 1‰) cannot be explained by a change of forsterite content alone.

Common crystallization differentiation is accompanied by the negative correlation between $\delta^{18}O$ and Mg-number of olivine owing to the simultaneous decrease of Mg-number and an increase of melt $\delta^{18}O$ via the removal of olivine (Genske et al., 2013). The positive correlation of these values (usually expressed in decreasing olivine $\delta^{18}O$ in more evolved rock varieties) is frequently explained by the contamination of mantle melts with low-$\delta^{18}O$ hydrothermally altered material in the melt generation zone. Corresponding geological models involve isotopically light material in the generation of magmatic melts either in magma chamber or beyond it (Bindeman et al., 2008; Cheong et al., 2017).

For Changbaishan volcano, the contribution of low-^{18}O material was proposed to explain the low $\delta^{18}O$ in zircon from 946 A.D. lava eruptions (from 3.69 to 5.03‰, Cheong et al., 2017). The authors considered two variants: melting of hydrothermally altered stagnant slab and "absorption" of previously crystallized hydrothermally reworked walls by melts supplying in a chamber. However, the cited work discussed only isotope data on zircon, whereas $\delta^{18}O$ in the groundmass was not studied. The oxygen isotope data on zircon are insufficient to substantiate the involvement of material with anomalous oxygen composition in melt generation.

Our data are inconsistent with idea of contamination of Changbaishan lavas with low-$\delta^{18}O$ material, as follows from the measured $\delta^{18}O$ values in rock matrix (($\delta^{18}O(m)$ increases from 5.64 to 7.09‰). Thereby, the low $\delta^{18}O$ values were found only in the olivine phenocrysts from felsic lavas, whereas olivine from alkali basalts have normal (mantle) $\delta^{18}O(Ol)$ values. Low $\delta^{18}O$ values were not also found among numerous oxygen isotope determinations in bulk lava samples of Changbaishan volcano (Sakhno, 2007). It is highly possible that data obtained on zircon (Cheong et al., 2017) mark the same processes of the disturbance of phenocryst-melt oxygen isotope equilibrium as are discussed in this work for olivine.

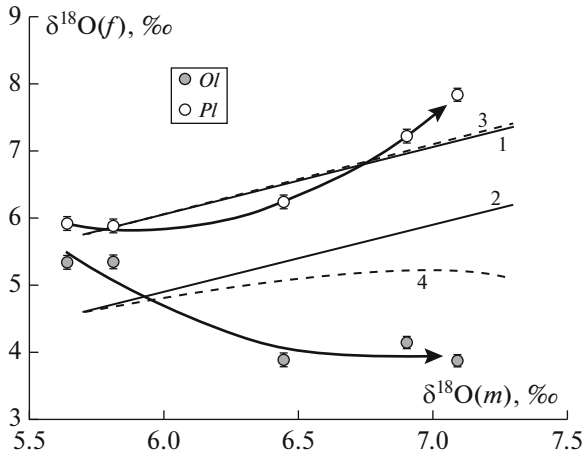

Fig. 5. Oxygen isotope composition of phenocrysts ($\delta^{18}O(f)$) vs. oxygen isotope composition of groundmass ($\delta^{18}O(m)$). Lines with arrows show the observed evolution of isotope parameters of olivine and plagioclase phenocrysts with differentiation of melts of Changbaishan volcano. Calculated lines show the complete O-isotope equilibrium with melt of: (1) plagioclase, (2) olivine. Dashed line shows calculated variations of $\delta^{18}O$ in phenocrysts, which met local isotope equilibrium but did not reach volume diffusion isotope equilibration with melt: (3) calculation for plagioclase; (4) for olivine (see text). In calculations, the linear change of $\delta^{18}O(m)$ and olivine–plagioclase mass proportions was given from $\{X_{Ol} = 0.6, X_{Pl} = 0.4\}$ in alkali basalts to $\{X_{Ol} = 0.1, X_{Pl} = 0.9\}$ in alkali rhyolites. The values of olivine–melt and plagioclase–melt isotope fractionation were taken constant and equal (−1.1‰) and (−0.1‰), respectively. The measurement error of $\delta^{18}O$ is no more than the symbol size in the diagram.

The Degree of Polymerization and Oxygen Isotope Composition of Melts

An increase of $\delta^{18}O$ value in the groundmass is likely related to the crystallization differentiation and is accompanied by a change of not only chemical composition of melts, but also the degree of their polymerization. The degree of melt polymerization is expressed by the NBO/T ratio, i.e., the ratio of non–bridging oxygens to tetrahedral cations (Mysen, 1997; Mysen et al., 1985; Mysen and Richet, 2005). As shown experimentally, silicate melts have different ability to concentrate heavy oxygen isotope ^{18}O depending on the degree of polymerization (Dubinina and Borisov, 2018), and the oxygen isotope shift relative to the reference phase is inversely proportional to

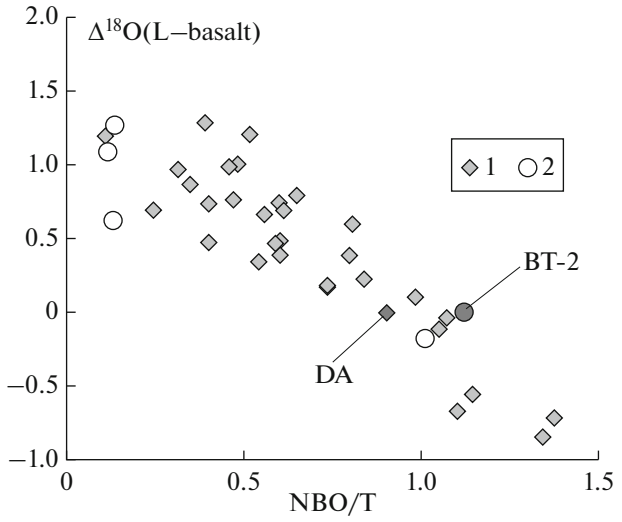

Fig. 6. Oxygen isotope fractionation in melts depending on NBO/T ratio: (1) experimental data on the oxygen isotope fractionation in silicate melts relative to haplobasalt (DA) at 1500°C (Dubinina and Borisov, 2018); (2) oxygen isotope fractionation in lavas of Changbaishan volcano relative to trachybasalt sample BT-2.

the NBO/T ratio. In other words, the higher the degree of melt polymerization, the greater is the ^{18}O concentration in the melt relative to the same reference phase (melt or mineral).

The Changbaishan lavas linked by a single crystallization event show a wide compositional range. Hence, the degree of polymerization (NBO/T) varies by almost an order of magnitude: from 0.112 in the alkaline salic varieties to 1.118 in the alkali basalts (Table 1). Taking sample of the least polymerized trachybasaltic andesite with the highest NBO/T = 1.118 (sample BT-2 in Table 1) as the reference phase, data on other lavas can be compared with experimental dependence (Dubinina and Borisov, 2018). Figure 6 demonstrates the values of oxygen isotope shift in lavas of Changbaishan volcano relative to sample BT-2. For comparison, the diagram also shows experimental data, where isotope shift was calculated relative to a haplobasaltic melt having NBO/T = 0.91 (Dubinina and Borisov, 2018), which is close to that of sample BT-2. Experimental points in the diagram Δ_{L-DA}–NBO/T (Fig. 6) are approximated by the linear equation:

$$\Delta_{L-DA} = -1.5(\pm 0.36)\left(\frac{NBO}{T}\right) + 1.4(\pm 0.35), \quad (6)$$

where Δ_{L-DA} is the difference between $\delta^{18}O$ in a silicate melt and in a diopside–anorthite (DA) eutectic melt, which served as the reference phase in experiment (Dubinina and Borisov, 2018).

It is seen from comparison that the natural lavas of Changbaishan volcano fall within the experimental trend in Fig. 6. However, such indirect comparison is arbitrary, because estimated temperatures of rock formation (700–1200°C, Andreeva et al., 2018) differ from experimental temperature (1500°C, Dubinina and Borisov, 2018). In addition, the experiments studied the alkali–free compositions, whereas all studied rocks of Changbaishan volcano are derivatives of alkaline series. It should be noted that the observed agreement between natural and experimental data additionally supports that the end derivatives of alkali lavas of Changbaishan volcano were derived from a common magmatic melt and that the volcano magma did not experience significant contamination during differentiation.

Influence of the Degree of Melt Polymerization on the Oxygen Isotope Composition of Phenocrysts

As follows from above considerations, neither change of olivine Mg-number nor local–equilibrium disturbance of oxygen isotope equilibrium can explain a 1.5‰ decrease of $\delta^{18}O(Ol)$ from alkali basalts to felsic varieties. Indeed, with allowance for a change of $\delta^{18}O(m)$, the difference in oxygen isotope composition of olivine between end–member rocks is about 3‰. This is a very large shift for olivine and suggests the influence of additional factors. Among these factors could be the kinetic isotope effect (KIE) caused by the rapid crystallilzation of the mineral. The preservation of kinetic isotope shift is more probable in minerals with low oxygen diffusion rate. At first glance, this could explain the disequilibrium relations of $\delta^{18}O$ values in the olivine–melt system and insignificant deviations from equilibrium in the plagioclase–melt system found in lavas of Changbaishan volcano. KIE should cause a shift toward the lower $\delta^{18}O$ values of phenocryst relative to the expected equilibrium composition. However, the fractionation between olivine and melt deviates in both sides from the inferred equilibrium value (Fig. 4). It is hardly probable that KIE occurred only in the olivine–alkaline rhyolite system and did not affect the olivine–alkali basalt system. In contrast, the less viscous alkali basalts have the higher crystallization rates. Hence, the KIE occurrence in them is more probable.

As compared to the olivine Mg-number, the degree of melt polymerization oxygen isotope can have a stronger effect on the olivine–melt oxygen isotope fractionation coefficient. However, this parameter is ignored in standard temperature dependences for calculating the fractionation factors and in the existing melt approximation methods. Experimental dependences obtained within a wide NBO/T range allowed us to estimate the direction and value of oxygen isotope shift between two melts (Borisov and Dubinina, 2014; Dubinina and Borisov, 2018). These data cannot be applied to the mineral–melt system owing to the absence of corresponding experimental calibrations.

However, the direction and scale of isotope shifts in the mineral phenocrysts in response to a change of the degree of melt polymerization can be estimated to a first approximation. To this end, we applied the experimental dependence of oxygen isotope shift between melts on NBO/T described by Eq. (6). To pass to the mineral–melt system, it was assumed that quartz and silica melt are equally able to concentrate ^{18}O. This assumption is arbitrary, because the experimental study of the SiO_2-glass exchange with CO_2 at 550–950°C (Stolper and Epstein, 1991) showed that the silica glass is enriched by 0.3–0.6‰ relative to crystalline quartz. Nevertheless, this effect can be ignored because these calculations are only approximate. Quartz is suitable since represents a phase with zero NBO/T ratio, since it contains only oxygen bonded to tetrahedral silica cations. According to Eq. (6), the isotope oxygen shift between quartz and DA melt (Δ_{Qz-DA}) should be about 1.4‰, i.e.,

$$\delta_{DA} = \delta_{Qz} - 1.4. \quad (7)$$

Combining Eqs. (6) and (7) gives an expression describing the dependence of the oxygen isotope composition on melt $\delta^{18}O$ (δ_L) and the degree of its polymerization, $(NBO/T)_L$:

$$\delta_{Qz} = \delta_L + 1.5\left(\frac{NBO}{T}\right)_L. \quad (8)$$

Further, we may apply any known quartz–mineral temperature dependences, for instance consistent equations for high-temperature (>600°C) equilibria (Chacko et al., 2001; Valley, 2003), which in general view can be written as follows:

$$10^3 \ln\alpha(Qz - Min) = A_{Qz-Min} \times 10^6 T^{-2} \approx \delta_{Qz} - \delta_{Min}, \quad (9)$$

where A_{Qz-Min} is the corresponding coefficient of thermometric equation, T is the absolute temperature (K). Combining equations (8) and (9) gives equations for calculating the oxygen isotope composition of mineral in equilibrium with a melt, if temperature, NBO/T ratio, and oxygen isotope composition of melt (δ_L) are known:

$$\delta_{Min} = \delta_L - 10^3 \ln\alpha(Qz - Min) + 1.5\left(\frac{NBO}{T}\right). \quad (10)$$

For each studied lava sample, the oxygen isotope compositions of olivine and plagioclase phenocrysts were calculated using Eq. (10) at temperatures presented in Table 2. The $\delta^{18}O(Ol)$ and $\delta^{18}O(Pl)$ values were calculated using temperature dependences for mineral pairs *Qz–Ab*, *Qz–An,* and *Qz–Fo* (Chacko et al., 1989), with correction for fayalite content in olivine introduced according to (Zheng, 1993). Calculation results shown in Fig. 7 correspond to the observed oxygen isotope relations between olivine phenocrysts and the groundmass of studied lavas. Some deviations from observed $\delta^{18}O$ values could be caused by several reasons: the conditionality of values estimated from Eq. (5), the possible errors in temperatures estimated from melt inclusions, as well as the formalism of the NBO/T calculation, especially for felsic alkaline melts (Mysen et al., 1985; Mysen, 1990, 1997; Mysen and Richet, 2005). In addition, experimental data were obtained for the alkali-free system (Dubinina and Borisov, 2018; Borisov and Dubinina, 2014), whereas all studied samples are alkaline rocks. Nevertheless, the alkali basalts show a good agreement between calculated and measured $\delta^{18}O(Ol)$ and $\delta^{18}O(Pl)$ values. In the range of alkaline salic compositions, the scatter in the estimates is much higher. However, the main conclusion drawn from this calculation is that the low (up to 3‰) $\delta^{18}O$ values in Fe–rich olivine from alkaline–salic lavas of Changbaishan volcano and the positive correlation between olivine $\delta^{18}O$ and its Mg-number (Fig. 7b) could be explained by the change of the degree of melt polymerization during crystallization differentiation.

CONCLUSIONS

The study of oxygen isotope composition in the differentiated alkaline rocks of Changbaishan volcano shows that the oxygen isotope equilibration in the phenocryst–melt system in rapidly cooling rocks cannot be described by simple models. According to the existing concepts of equilibrium oxygen isotope fractionation in the phenocryst–melt system (e.g., Zheng, 2003), the plagioclase phenocrysts in lavas of Changbaishan volcano are close to the oxygen isotopic equilibrium with the groundmass or melts, which was provided by the high oxygen diffusion rate in plagioclase. Olivine phenocrysts, in contrast, were crystallized far from oxygen isotope equilibrium with groundmass or melt. Based on the known values of oxygen isotope fractionation in the olivine–melt system (Zhao and Zheng, 2003), it is necessary to accept that olivine crystallization was accompanied by kinetic isotope effect, which later was not compensated by the diffusion exchange with surrounding groundmass or melt owing to the low oxygen diffusion rate in olivine. Such mechanism is possible, but some features of the oxygen isotope partitioning between groundmass and olivine are inconsistent with the concept of kinetic isotope effect.

An alternative approach for estimating the oxygen isotope equilibrium between phenocrysts and melts is to involve the melt polymerization. This approach suggests that the oxygen isotope fractionation in the phenocryst–melt system can be described by equation containing two terms: quartz–mineral fractionation coefficient ($\alpha(Qz–Min)$) and the degree of melt polymerization expressed through NBO/T ratio. The first term is sensitive to temperature, while the second, to the chemical composition and structure of silicate

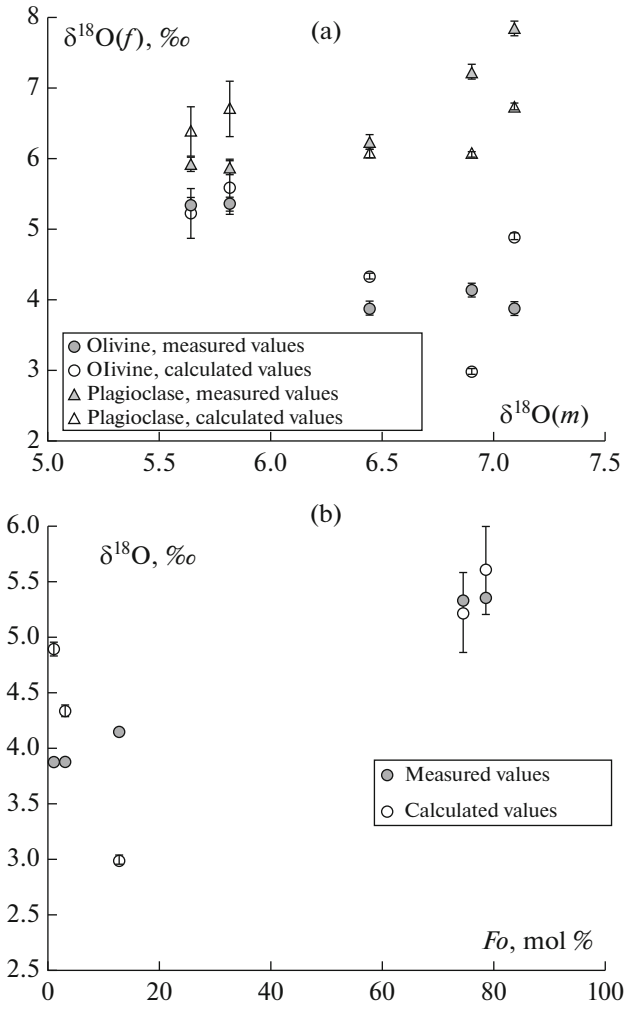

Fig. 7. Oxygen isotope composition in olivine and plagioclase phenocrysts in lavas of Changbaishan volcano depending on the oxygen isotope composition of the groundmass (a) and correlation between $\delta^{18}O$ and olivine Mg-number (b). Calculation was carried out using Eq. (5) based on the experimental dependence of oxygen isotope shift between silicate melts versus NBO/T ratio (Dubinina and Borisov, 2018), see text. Measurement error of $\delta^{18}O$ and olivine Mg-number is no more than symbol size in the diagram, vertical error bars are shown according to variations of angular coefficient in Eq. (6).

melt. It is possible that this approach will be universal for estimating the oxygen isotope fractionation in the mineral–melt system, but its further development requires the incorporation of the corresponding coefficients or terms, which take into account the temperature and pressure dependence of NBO/T.

A proposed approach can be applied to solving petrological problems using the isotope–geochemical composition of olivine, as well as zircon, which has the high fractionation coefficient with quartz (Valley et al., 2003; Qin et al., 2016). An equation proposed for calculating the influence of the degree of melt polymerization on phenocryst $\delta^{18}O$ shows that the maximum isotope effects are inferred in minerals having the high fractionation coefficient with quartz. The occurrence of these effects is provoked by the high degree of melt polymerization (i.e., low NBO/T). During crystallization of minerals having the low fractionation coefficient with quartz (sodic plagioclases, light micas), which is usually observed in the low-NBO/T felsic melts, the correction for NBO/T will be insignificant. Based on the sign of this correction, it can be predicted, for instance, that the $\delta^{18}O$ value of plagioclase phenocrysts could become higher than inferred equilibrium values with decreasing the degree of melt polymerization.

A positive correlation between $\delta^{18}O$ of olivine and its Mg-number in lavas of Changbaishan volcano can be explained by variations in the degree of melt polymerization during differentiation. Moreover, the observed decrease of $\delta^{18}O$ in Fe-rich olivine from alkaline–salic lavas of the volcano seems quite logical in the framework of the proposed approach. Based on obtained conclusions, complex geological models that imply the involvement of low-$\delta^{18}O$ material or episodes of hydrothermal activity during the generation of magmatic melts of Changbaishan volcano can be ruled out.

ACKNOWLEDGMENTS

We are grateful to reviewers for relevant comments, which significantly improved this paper.

FUNDING

This work was financially supported by the Russian Science Foundation (project no. 18-17-00126). Petrographic and mineralogical study was carried out with the partial support by the RF President grant (MK-2419.2019.5).

REFERENCES

Andreeva, O.A., Yarmolyuk, V.V., Andreeva, I.A., et al. The composition and sources of magmas of Changbaishan Tianchi Volcano (China–North Korea), *Dokl. Earth Sci.,* 2014, vol. 456, no. 2, pp. 572–578.

Andreeva, O.A., Yarmolyuk, V.V., Andreeva, I.A., and Borisovskii, S.E., Magmatic evolution of Changbaishan Tianchi Volcano, China–North Korea: evidence from mineral-hosted melt and fluid inclusions, *Petrology,* 2018, vol. 26, no. 5, pp. 515–545.

Appora, I., Eiler, J.M., Matthews, A., and Stolper, E.M., Experimental determination of oxygen isotope fractionations between CO_2 vapor and soda–melilite melt, *Geochim. Cosmochim. Acta,* 2003, vol. 67, pp. 459–471.

Ariskin, A.A. and Polyakov, V.B., Simulation of molecular mass distributions and evaluation of O^{2-} concentrations in polymerized silicate melts, *Geochem. Int.,* 2008, vol. 46, no. 5, pp. 429–447.

Bigeleisen, J. and Mayer, M.G., Calculation of equilibrium constants for isotope exchange reactions, *J. Chem. Phys.,* 1947, vol. 15, pp. 261–267.

Bindeman, I., Gurenko, A., Sigmarsson, O., and Chaussidon, M., Oxygen isotope heterogeneity and disequilibria of olivine crystals in large volume Holocene basalts from Iceland: evidence for magmatic digestion and erosion of Pleistocene hyaloclastites, *Geochim. Cosmochim. Acta,* 2008, vol. 72, pp. 4397–4420.

Borisov, A.A. and Dubinina, E.O., Effect of network-forming cations on the oxygen isotope fractionation between silicate melts: experimental study at 1400–1570C, *Petrology,* 2014, vol. 22, no. 4, pp. 359–380.

Bucholz, C.E., Jagoutz, O., Van Tongeren, J.A., et al., Oxygen isotope trajectories of crystallizing melts: insights from modeling and the plutonic record, *Geochim. Cosmochim. Acta,* 2017, vol. 207, pp. 154–184.

Chacko, T., Cole, D.R., and Horita, J., Equilibrium oxygen, hydrogen and carbon isotope fractionation factors applicable to geological systems, *Rev. Mineral. Geochem.,* 2001, vol. 43, pp. 1–81.

Chakraborty, S., Diffusion coefficients in olivine, wadsleyite and ringwoodite, *Rev. Mineral. Geochem.,* 2010, vol. 72, pp. 603–639.

Cheong, A.C., Sohn, Y.K., Jeong, Y.-J., et al., Latest Pleistocene crustal cannibalization at Baekdusan (Changbaishan) as traced by oxygen isotopes of zircon from the millennium eruption, *Lithos,* 2017, vol. 284-285, pp. 132–137.

Cherniak, D.J. and Watson, E.B., Diffusion in zircon, *Rev. Mineral. Geochem.,* 2003, vol. 53, no. 1, pp. 113–143.

Clayton, R.N. and Kieffer, S.W., Oxygen isotope thermometer calibrations, *Stable Isotope Geochemistry: A Tribute to Samuel Epstein*, Taylor, H.P.Jr., O'Neil, J.R., and Kaplan, I.R., Eds., *Geochem. Soc. Spec. Publ.,* 1991, no. 3, pp. 3–10.

Day, J.M.D., Peters, B.J., and Janney, P.E., Oxygen isotope systematics of South African olivine melilitites and implications for HIMU mantle reservoirs, *Lithos,* 2014, vol. 202–203, pp. 76–84.

DePaolo, D.J., Trace element and isotopic effects of combined wall-rock assimilation and fractional crystallization, *Earth Planet. Sci. Lett.,* 1981, vol. 53, pp. 189–202.

Dodson, M.H., Closure temperature in cooling geochronological and petrological systems, *Contrib. Mineral. Petrol.,* 1973, vol. 40, pp. 259–274.

Dubinina, E.O. and Borisov, A.A., Structure and composition effects on the oxygen isotope fractionation in silicate melts, *Petrology,* 2018, vol. 26, no. 4, pp. 414–427.

Dubinina, E.O. and Lakshtanov, L.Z., A kinetic model of exchange in dissolution–precipitation processes, *Geochim. Cosmochim. Acta,* 1997, vol. 61, pp. 2265–2273.

Dubinina, E.O., Nosova, A.A., Avdeenko, A.S., and Aranovich, L.Ya., Isotopic (Sr, Nd, O) systematics of the high Sr–Ba Late Miocene granitoid intrusions from the Caucasian Mineral Waters region, *Petrology,* 2010, vol. 18, no. 3, pp. 211–238.

Dubinina, E.O., Aranovich, L.Y., van Reenen, D.D., et al., Involvement of fluids in the metamorphic processes within different zones of the southern marginal zone of the Limpopo Complex, South Africa: an oxygen isotope perspective, *Precambrian Res.,* 2015, vol. 256, pp. 48–61.

Eiler, J.M., Oxygen isotope variations of basaltic lavas and upper mantle rocks, *Rev. Mineral. Geochem.,* 2001, vol. 43, pp. 319–364.

Fan, Q., Sui, J.L., Wang, T.H., et al., History of volcanic activity, magma evolution and eruptive mechanisms of the Changbai volcanic province, *Geol. J. China Univer.,* 2007, no. 13, pp. 175–190.

Farver, J.R., Oxygen and hydrogen diffusion in minerals, *Rev. Mineral. Geochem.,* 2010, vol. 72, no. 1, pp. 447–507.

Farver, J.R. and Yund, R.A., The effect of hydrogen, oxygen, and water fugacity on oxygen diffusion in alkali feldspar, *Geochim. Cosmochim. Acta,* 1990, vol. 54, pp. 2953–2964.

Garlick, G.D., Oxygen isotope fractionation in magmatic rocks, *Earth Planet. Sci. Lett.,* 1966, vol. 1, pp. 361–368.

Genske, F.S., Beier, C., Haase, K.M., et al., Oxygen isotopes in the azores islands: crustal assimilation recorded in olivine, *Geology,* 2013, vol. 41, pp. 491–494.

Gérard, O. and Jaoul, O., Oxygen diffusion in olivine, *J. Geophys. Res. Atmospheres,* 1989, vol. 94 V, no. B4, pp. 4119–4128.

Giletti, B.J., Diffusion effects on oxygen isotope temperatures of slowly cooled igneous and metamorphic rocks, *Earth Planet. Sci. Lett.,* 1986, vol. 77, pp. 218–228.

Giletti, B.J., Semet, M.P., and Yund, R.A., Studies in diffusion-III. Oxygen in feldspars: an ion microprobe determination, *Geochim. Cosmochim. Acta,* 1978, vol. 42, pp. 45–57.

Günther, T., Haase, K.M., Junge, M., et al., Oxygen isotope and trace element compositions of platiniferous dunite pipes of the Bushveld Complex, South Africa—signals from a recycled mantle component?, *Lithos,* 2018, vol. 310–311, pp. 332–341.

Hsu, Ch.-N., Chen, J.-Ch., and Ho, K.-S., Geochemistry of Cenozoic volcanic rocks from Kirin Province, northeast China, *Geochem. J.,* 2000, vol. 34, pp. 33–58.

Jaoul, O., Froidevaux, C., Durham, W.B., and Michaut, M., Oxygen self-diffusion in forsterite: implications for the high temperature creep mechanism, *Earth Planet. Sci. Lett.,* 1980, vol. 47, pp. 613–624.

Kalamarides, R.I., High-temperature oxygen isotope fractionation among the phases of the Kiglapait intrusion, Labrador, Canada, *Chem. Geol.,* 1986, vol. 58, pp. 303–310.

Kuritani, T., Ohtani, E., and Kimura, J.I., Intensive hydration of the mantle transition zone beneath China caused by ancient slab stagnation, *Nature Geosci.,* 2011, vol. 4, pp. 713–716.

Kyser, T.K., Lesher, C.E., and Walker, D., The effects of liquid immiscibility and thermal diffusion on oxygen isotopes in silicate liquids, *Contrib. Mineral. Petrol.,* 1998, vol. 133, pp. 373–381.

Lesher, C.E., Self-diffusion in silicate melts: theory, observations and applications to magmatic systems, *Rev. Mineral. Geochem.,* 2010, vol. 72, pp. 269–309.

Lester, G.W., Kyser, T.K., and Clark, A.H., Oxygen isotope partitioning between immiscible silicate melts with H_2O, P and S, *Geochim. Cosmochim. Acta,* 2013, vol. 109, pp. 306–311.

Liu, J., Chen, Sh.-Sh., Guo, Zh., et al., Geological background and geodynamic mechanism of Mt. Changbai vol-

canoes on the China–Korea border, *Lithos,* 2015, vol. 236–237, pp. 46–73.

Liu, R., Fan, Q., Zheng, X., et al., The magma evolution of Tianchi volcano, Changbaishan, *Sci. China,* 1998, vol. 41, no. 4, pp. 382–389.

Mattey, D., Lowry, D., and Macpherson, C., Oxygen isotope composition of mantle peridotite, *Earth Planet. Sci. Lett.,* 1994, vol. 128, pp. 231–241.

Matthews, A., Palin, J.M., Epstein, S., and Stolper, E.M., Experimental study of $^{18}O/^{16}O$ partitioning between crystalline albite, albitic glass and CO_2 gas, *Geochim. Cosmochim. Acta,* 1994, vol. 58, pp. 5255–5266.

Muehlenbachs, K. and Kushiro, I., Oxygen isotope exchange and equilibrium of silicates with CO_2 and O_2, *Carnegie Inst. Wash. Yearbook,* 1974, vol. 73, pp. 232–236.

Mysen, B.O., Relationships between silicate melt structure and petrologic processes, *Earth Sci. Rev.,* 1990, vol. 27, pp. 281–365.

Mysen, B.O., Aluminosilicate melts: structure, composition and temperature, *Contrib. Mineral. Petrol.,* 1997, vol. 127, pp. 104–118.

Mysen, B.O. and Richet, P., *Silicate Glasses and Melts: Properties and Structure*, Amsterdam: Elsevier, 2005.

Mysen, B.O., Virgo, D., and Seifert, F.A., Relationships between properties and structure of aluminosilicate melts, *Am. Mineral.,* 1985, vol. 70, pp. 88–105.

Nardini, I., Armienti, P., Rocchi, S., et al., Sr-Nd-Pb-He-O isotope and geochemical constraints on the genesis of Cenozoic magmas from the West Antarctic rift, *J. Petrol.,* 2009, vol. 50, no. 7, pp. 1359–1375.

Oppenheimer, C., Wacker, L., Xu, J., et al., Multi-proxy dating the "millenium" eruption of Changbaishan to late 946 CE, *Quatern. Sci. Rev.,* 2017, vol. 158, pp. 164–171.

Palin, J.M., Epstein, S., and Stolper, E., Oxygen isotope partitioning between rhyolitic glass/melt and CO_2: an experimental study at 550–950°C and 1 bar, *Geochim. Cosmochim. Acta,* 1996, vol. 60, pp. 1963–1973.

Qin, T., Wu, F., Wu, Z., and Huang, F., First principles calculations of equilibrium fractionation of O and Si isotopes in quartz, albite, anorthite and zircon, *Contrib. Mineral. Petrol.,* 2016, vol. 171, p. 91.

Sakhno, V.G., Chronology of eruptions, composition, and magmatic evolution of the Paektusan Volcano: evidence from K–Ar, $^{87}Sr/^{86}Sr$, and $\delta^{18}O$ isotope data, *Dokl. Earth Sci.,* 2007, vol. 412, no. 2, pp. 22–28.

Sakhno, V.G., *Noveishii i sovremennyi vulkanizm Yuga Dal'nego Vostoka* (The Youngerst and Modern Volcanism of the Southern Far East), Vladivostok: Dal'nauka, 2008.

Sharp, Z.D., A laser-based microanalytical method for the in situ determination of oxygen isotope ratios in silicates and oxides, *Geochim. Cosmochim. Acta,* 1990, vol. 54, pp. 1353–1357.

Stolper, E. and Epstein, S., An experimental study of oxygen isotope partitioning between silica glass and CO_2 vapor, *Stable Isotope Geochemistry: A Tribute to Samuel Epstein*, Taylor, H.P., Jr., O'Neil, J.R., and Kaplan, I.R., Eds., *Geochem. Soc. Sp. Publ.,* 1991, vol. 3, pp. 35–51.

Taylor, H.P., The effects of assimilation of country rocks by magmas on $^{18}O/^{16}O$ and $^{87}Sr/^{86}Sr$ systematic in igneous rocks, *Geotektonika,* 1980, vol. 47, pp. 243–254.

Valley, J.W., Stable isotope thermometry at high temperatures, *Rev. Mineral. Geochem.,* 2001, vol. 43, pp. 365–414.

Valley, J.W., Oxygen isotopes in zircon, *Rev. Mineral. Geochem.,* 2003, vol. 53, no. 1, pp. 343–385.

Valley, J.W., Kitchen, N., Kohn, M.J., et al., UWG-2, a garnet standard for oxygen isotope ratios: strategies for high precision and accuracy with laser heating, *Geochim. Cosmochim. Acta,* 1995, vol. 59, pp. 5223–5231.

Wang, X.-C., Wilde, S.A., Qiu-Li, Li., and Ya-Nan, Yang., Continental flood basalts derived from the hydrous mantle transition zone, *Nature Commun.,* 2015, vol. 6, p. 7700.

Wei, H., Taniguchi, H., Miyamoto, T., et al., Stratigraphic sequences and magmatic cycles of the Tianchi volcano, Changbaishan, *Northeast Asian Studies,* 2007a, vol. 11, pp. 173–193.

Wei, H., Wang, Y., Jin, J., et al., Timescale and evolution of the intracontinental Tianchi volcanic shield and ignimbrite-forming eruption, Changbaishan, northeast China, *Lithos,* 2007b, vol. 96, vol. 1–2, pp. 315–324.

Yarmolyuk, V.V., Kudryashova, E.A., Kozlovskii, A.M., et al., Late Cenozoic volcanic province in Central and East Asia, *Petrology,* 2011, vol. 11, no. 4, pp. 327–347.

Zhao, Z.F. and Zheng, Y.F., Calculation of oxygen isotope fractionation in magmatic rocks, *Chem. Geol.,* 2003, vol. 193, pp. 59–80.

Zheng, Y.F., Calculation of oxygen isotope fractionation in anhydrous silicate minerals, *Geochim. Cosmochim. Acta,* 1993, vol. 57, pp. 1079–1091.

Translated by M. Bogina